Free Radical Biology and Medicine 164 (2021) 258–270

Contents lists available at ScienceDirect

Free Radical Biology and Medicine

journal homepage: www.elsevier.com/locate/freeradbiomed

Original article

Antioxidant function of phytocannabinoids: Molecular basis of their stability and cytoprotective properties under UV-irradiation

Jan Vacek [a,*], Jitka Vostalova [a], Barbora Papouskova [b], Denisa Skarupova [a], Martin Kos [c], Martin Kabelac [d], Jan Storch [c,**]

[a] Department of Medical Chemistry and Biochemistry, Faculty of Medicine and Dentistry, Palacky University, Hnevotinska 3, 775 15, Olomouc, Czech Republic
[b] Department of Analytical Chemistry, Faculty of Science, Palacky University, 17. Listopadu 12, 771 46, Olomouc, Czech Republic
[c] Department of Advanced Materials and Organic Synthesis, Institute of Chemical Process Fundamentals of the Czech Academy of Sciences, v. v. i., Rozvojova 135, 165 02, Prague 6, Czech Republic
[d] Department of Chemistry, Faculty of Science, University of South Bohemia, Branisovska 31, 370 05, Ceske Budejovice, Czech Republic

ARTICLE INFO

Keywords:
Phytocannabinoids
(photo)stability
Oxidation
Electronic structure
UVA/UVB photoprotection
Keratinocytes
Dermal fibroblasts

ABSTRACT

In this contribution, a comprehensive study of the redox transformation, electronic structure, stability and photoprotective properties of phytocannabinoids is presented. The non-psychotropic cannabidiol (CBD), cannabigerol (CBG), cannabinol (CBN), cannabichromene (CBC), and psychotropic tetrahydrocannabinol (THC) isomers and iso-THC were included in the study. The results show that under aqueous ambient conditions at pH 7.4, non-psychotropic cannabinoids are slight or moderate electron-donors and they are relatively stable, in the following order: CBD > CBG ≥ CBN > CBC. In contrast, psychotropic Δ^9-THC degrades approximately one order of magnitude faster than CBD. The degradation (oxidation) is associated with the transformation of OH groups and changes in the double-bond system of the investigated molecules. The satisfactory stability of cannabinoids is associated with the fact that their OH groups are fully protonated at pH 7.4 (*p*Ka is ≥ 9). The instability of CBN and CBC was accelerated after exposure to UVA radiation, with CBD (or CBG) being stable for up to 24 h. To support their topical applications, an *in vitro* dermatological comparative study of cytotoxic, phototoxic and UVA or UVB photoprotective effects using normal human dermal fibroblasts (NHDF) and keratinocytes (HaCaT) was done. NHDF are approx. twice as sensitive to the cannabinoids' toxicity as HaCaT. Specifically, toxicity IC_{50} values for CBD after 24 h of incubation are 7.1 and 12.8 μM for NHDF and HaCaT, respectively. None of the studied cannabinoids were phototoxic. Extensive testing has shown that CBD is the most effective protectant against UVA radiation of the studied cannabinoids. For UVB radiation, CBN was the most effective. The results acquired could be used for further redox biology studies on phytocannabinoids and evaluations of their mechanism of action at the molecular level. Furthermore, the UVA and UVB photoprotectivity of phytocannabinoids could also be utilized in the development of new cannabinoid-based topical preparations.

1. Introduction

The endocannabinoid system is one of the major receptor-driven mechanisms leading to the maintenance of homeostasis. We currently have relatively extensive knowledge of the structure and function of the two cannabinoid receptors, CB_1 and CB_2, which play a key role in the endocannabinoid system. Clearly the best known exogenous cannabinoid receptor ligands are phytocannabinoids, which are lipophilic phenolic terpenoids that have been isolated from *Cannabis sativa* [1,2]. The main phytocannabinoid is THC, Δ^9-tetrahydrocannabinol (Scheme 1), whose application leads not only to modulation of the endocannabinoid system, but also manifests a psychotropic effect [3].

C. sativa contains more than 180 phytocannabinoids, with pharmacological effects observed for many of them. In this sense, cannabidiol (CBD) is probably the best known member of the group of so-called non-psychotropic cannabinoids [4,5], without adverse effects associated with abuse, nor of prolonged use producing behavioral change, memory loss or generally chronic intoxication. Other intensively investigated

* Corresponding author.
** Corresponding author.
E-mail addresses: jan.vacek@upol.cz (J. Vacek), storchj@icpf.cas.cz (J. Storch).

https://doi.org/10.1016/j.freeradbiomed.2021.01.012
Received 29 September 2020; Received in revised form 10 December 2020; Accepted 6 January 2021
Available online 13 January 2021

phytocannabinoids include cannabinol, cannabichromene, cannabigerol (Scheme 1), or cannabivarin and their derivatives or analogues [3]. For more details on the phytochemical profile of *Cannabis sativa*, see Ref. [6].

From the point of view of the real application of phytocannabinoids, it is necessary to distinguish between the administration of a complex extract and the pure (isolated) substance. The application form also plays an important role. Phytocannabinoids are most commonly administered topically, orally, sublingually, rectally as suppositories or by inhalation [7]. When complex mixtures of phytocannabinoids are applied, synergistic or more often additive effects can be achieved compared to the application of only one phytocannabinoid. It is important to note that phytocannabinoids do not only act by binding to cannabinoid receptors, but also modulate the function of transient receptor potential (TRP) channels, peroxisome proliferator-activated receptor gamma (PPARγ), cyclooxygenase-2 (COX-2), etc., and are involved in calcium homeostasis. The pleiotropic, not exclusively receptor-driven, actions of phytocannabinoids are frequently discussed today [8].

In the development of new drugs, the synthetic THC analogue nabilone (marketed as Cesamet) has been applied for the treatment of nausea and vomiting associated with cancer chemotherapy. Similarly, dronabinol (or Marinol) has been introduced into clinical practice as an anti-emetic agent and later as an appetite stimulant. Probably the best known cannabinoid-based drug is known as nabiximols (trade name Sativex), which is a mixture of THC and CBD. Recently, a CBD antiepileptic drug known as Epidiolex has also been approved by the FDA. The extensive testing of CBD's safety and its introduction into the category of drugs opens up a wide field for other preparations containing non-psychotropic cannabinoids [3,9,10]. In recent decades, attention has also been paid to the development of synthetic derivatives, CB receptor agonists/antagonists and modulators [3]. In addition, phytocannabinoids are also used in the development of new medical devices, cosmetics or in the development of dietary supplements and in other selected applications for prophylaxis and complementary therapy. Based on our knowledge of natural cannabinoids, these substances can be used primarily in the fields of neurological therapy, chronic pain treatment, dermatology, complementary treatment for cancer therapy and eating disorders [11]. Their immunomodulatory and anti-inflammatory activities are promising properties of phytocannabinoids [10].

A great deal of attention has been paid to the *in vitro* evaluation of the effects of phytocannabinoids, often without describing their mode of action at the molecular level. Besides this, it is important to note that there is limited number of highly valuable mechanistic, pharmacological and clinical studies. As for the pleiotropic and biphasic mode of action and frequently discussed entourage effect of cannabinoids, the involvement of them in oxidative stress and cannabinoid-based antioxidant effects have recently begun to be discussed [12]. It was demonstrated that CBD protects the liver by inhibiting oxidative and nitrative stress [13] and attenuating inflammatory response [14]. In contrast, prooxidant effects of synthetic cannabinoids have been described [15]. An overview of the antioxidant action of CBD was recently reported [16]. However knowledge on the redox biology of other phytocannabinoids is very limited.

2. Material and methods

2.1. Chemicals and general methods

Cannabidiol (CBD) and cannabigerol (CBG) were purchased from CBDepot Ltd., both at 99% purity. Other commercially available reagent-grade materials were used as obtained from Sigma-Aldrich, Acros Organics, and TCI. All solvents (Lach-Ner) were of reagent grade and used without any further purification. Thin-layer chromatography (TLC) was performed on silica gel 60 F254-coated aluminum sheets, and compounds were visualized with UV light (254 nm) or phosphomolybdic acid. Column chromatography was performed using a Biotage HPFC system (Isolera One) with prepacked silica gel flash columns. The standard Schlenk technique was used for all reactions. ^{1}H and ^{13}C NMR spectra were recorded using a Bruker Avance at 400 MHz (^{1}H NMR) and 101 MHz (^{13}C NMR). Chemical shifts (δ) are reported in parts per million (ppm) relative to TMS, and referenced to residuals of $CDCl_3$

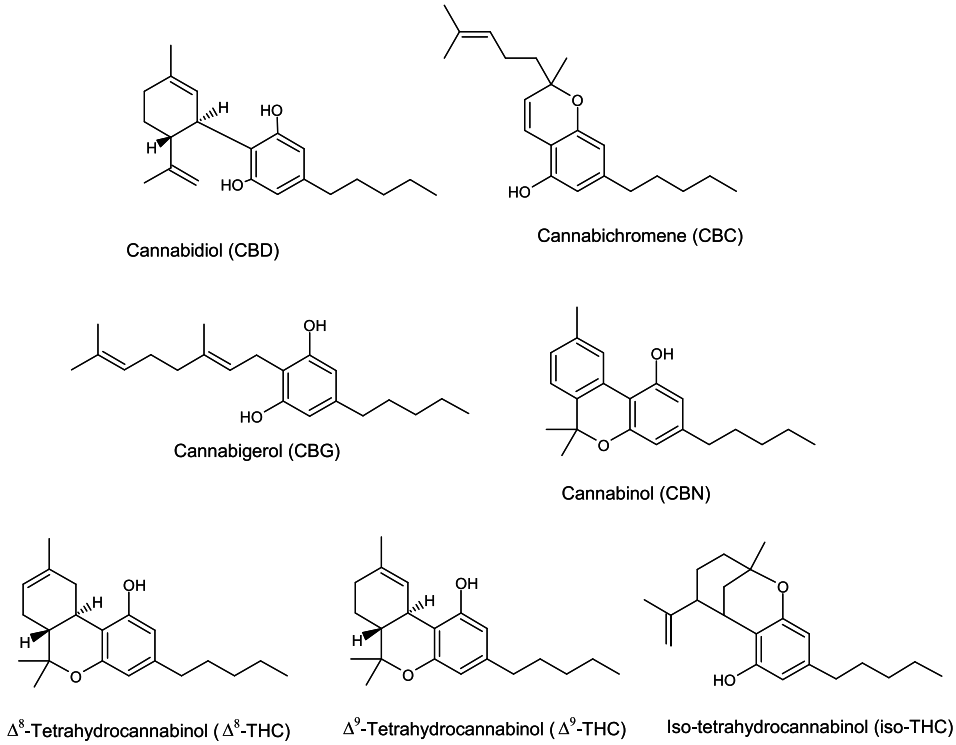

Scheme 1. Chemical structures of tested phytocannabinoids.

(δ = 7.26 and 77.00 ppm, respectively). The coupling constants (*J*) are given in Hertz (Hz) with corresponding multiplicity (s = singlet, d = doublet, t = triplet, q = quartet, m = multiplet).

2.1.1. Preparation of phytocannabinoids

Cannabichromene (CBC) [17] A 100 mL round-bottom flask equipped with a Dean-Stark trap was charged with 3.00 g (16.64 mmol) of olivetol, 2.99 mL (17.48 mmol) of citral, 1.76 mL (16.64 mmol) of *tert*-butylamine, and 33 mL of toluene. The reaction mixture was refluxed for 5 hours. After completion, the solvent was removed under reduced pressure. Flash chromatography using PE/EtOAc (95:5) provided 3.90 g (12.40 mmol, 74.5%) of CBC as a yellow oil (99% purity). NMR spectra were in accordance with published data [18].

Cannabinol (CBN) [19] A 100 mL round-bottom flask was charged with 2.00 g (6.36 mmol) of CBD, 3.23 g (12.72 mmol) of iodine, and 50 mL of toluene. The reaction mixture was refluxed for 7 hours. After completion, the mixture was washed with a saturated solution of $Na_2S_2O_3$ and brine. The organic phase was dried over anhydrous $MgSO_4$. After evaporation of the solvent, flash chromatography using PE/EtOAc (94:6) provided 0.69 g (2.22 mmol, 35%) of CBN as a yellow oil (99% purity). NMR spectra were in accordance with published data [20].

Δ^8-Tetrahydrocannabinol (Δ^8-THC) [21] A Schlenk flask was charged with 2.00 g (6.36 mmol) of CBD and 33 mL of DCM. The solution was cooled to 0 °C, and 0.32 mL (2.54 mmol) of $BF_3.Et_2O$ was added dropwise under an Ar atmosphere. The mixture was allowed to warm to r.t. After an additional hour of stirring, the mixture was poured into saturated $NaHCO_3$ and extracted with DCM. The combined organic phases were dried over anhydrous $MgSO_4$. After evaporation of the solvent, flash chromatography using pentane/Et_2O (95:5) provided 1.12 g (3.56 mmol, 56%) of Δ^8-THC as a yellow oil (99% purity). NMR spectra were in accordance with published data [21].

Δ^9-Tetrahydrocannabinol (Δ^9-THC) and **Δ^8-*iso*-tetrahydrocannabinol** (iso-THC) [22,23] A Schlenk flask was charged with 2.00 g (6.36 mmol) of CBD and 33 mL of DCM. The solution was cooled to −10 °C and 0.32 mL (2.54 mmol) of $BF_3.Et_2O$ was added dropwise under an Ar atmosphere. The mixture was stirred at −10 °C for 120 min. The reaction was quenched by the addition of saturated $NaHCO_3$. After extraction with DCM, the combined organic phases were dried over anhydrous $MgSO_4$. After evaporation of the solvent, flash chromatography using pentane/Et_2O (97:3) provided 1.04 g (3.31 mmol, 52%) of Δ^9-THC as a yellow oil (99% purity) and 156 mg (0.496 mmol, 7.8%) of iso-THC as a yellow oil (98% purity). NMR spectra of Δ^9-THC are in accordance with published data [24]. NMR spectra of iso-THC: ^{1}H NMR (400 MHz, $CDCl_3$) δ 6.28 (d, *J* = 1.5 Hz, 1H), 6.12 (d, *J* = 1.5 Hz, 1H), 4.99 (q, *J* = 1.5 Hz, 1H), 4.93 (s, 1H), 4.54 (s, 1H), 3.46 (q, *J* = 3.1 Hz, 1H), 2.51–2.40 (m, 2H), 2.34 (s, 1H), 1.93–1.83 (m, 4H), 1.80–1.53 (m, 7H), 1.42–1.21 (m, 7H), 0.92–0.86 (m, 3H). ^{13}C NMR (101 MHz, $CDCl_3$) δ 157.39, 152.25, 146.07, 142.62, 111.02, 110.78, 107.91, 105.98, 74.63, 43.03, 35.70, 35.45, 31.58, 30.76, 30.48, 29.41, 27.89, 22.65, 22.55, 21.05, 14.01; for more details, see Supplementary Information.

For *in vitro* cell experiments, methanol (HiPerSolv CHROMANORM for HPLC, LC-MS grade) was from VWR International s.r.o. (Czech Republic). Dulbecco's modified Eagle's medium (DMEM), Ham-F12 nutrient mixture, heat-inactivated fetal calf serum (FCS), stabilised penicillin-streptomycin solution, amphotericin B, hydrocortisone, adenine, insulin, epidermal growth factor, 3,3',5-triiodo-L-thyronine, trypsin, ampicillin, trypsin-EDTA (0.25%), dimethyl sulfoxide (DMSO), neutral red (NR), and other chemicals were from Sigma-Aldrich (Czech Republic).

2.2. Electrochemical measurement

The substances were analyzed using square-wave voltammetry (SWV) with the working electrode being a glassy carbon electrode (GCE, 1 mm diameter disc, BASi, USA). Before each electrochemical experiment, the GCE was polished using diamond spray (particle size was 3 μm) from Kernet Int. (UK). After polishing, the electrode was rinsed thoroughly with deionized water. The analyses were performed with Britton-Robinson buffer (titrated to the desired pH with 0.2 M NaOH) at room temperature with a μAutolab III analyzer (EcoChemie, NL) in a three-electrode setup with a Ag/AgCl/3 M KCl electrode as the reference and a platinum wire as the auxiliary electrode. Argon was used to remove oxygen from the supporting electrolyte. Individual settings for respective voltammetric analyses are given in the Figure legends.

2.3. Theoretical calculations

Since the cannabinoids are flexible molecules due to the presence of aliphatic side-chains, a two-stage Monte Carlo approach in the dihedral space implemented in the program FROG2 [25] was used as the first step in retrieving the energetically most stable structures of the given compounds. The twenty most favorable conformers found were further optimized at the DFT level of theory employing the 6-311++G(d, p) basis set and wB97XD functional, which provides reasonable geometries and thermodynamics data [26]. The frontier molecular orbitals and molecular electrostatic potentials were analyzed using the program Avogadro [27]. The presence of solvent (water, methanol and *n*-octanol) was described implicitly using the PCM model [28].

A harmonic vibrational frequency analysis was performed to confirm that the structures found are the minima at the potential energy surface. The vertical and adiabatic ionization potentials were calculated by subtracting the energies of the compound and its cation at the same level of theory as the previous *ab initio* calculations were performed. All quantum mechanical calculations were treated in the program Gaussian16 [29].

2.3.1. Dissociation of the cannabinoids

The calculations of pK_a were performed based on the procedure [30], where a corresponding thermodynamics cycle can be found, with the modification of Pliego [31]. Based on Eq. (1), the calculation of pK_a can be done through the following equations (2) and (3):

$$HA + H_2O \leftrightarrow A^- + H_3O^+ \quad (1)$$

$$\Delta G_g = G_g(A^-) + G_g(H_3O^+) - G_g(HA) - G_g(H_2O) \quad (2)$$

$$\Delta G = \Delta G_g + G_{solv}(A^-) + G_{solv}(H_3O^+) - G_{solv}(HA) - G_{solv}(H_2O) \quad (3)$$

Where G_g corresponds to the chemical potential of the given compound, and G_{solv} to its solvation free energy.

$$\text{Thus,} \quad pK_a = \frac{\Delta G}{RT} - \log[H_2O] \text{ with } [H_2O] = 55.49 \text{ mol/dm}^3. \quad (4)$$

Since the calculated solvation free energy of H_3O^+ is the main source of error in this approach, this value was replaced by an experimental one equal to −110.2 kcal/mol [31]. To minimize errors, the pK_a values obtained for HA *via* equation (4) were scaled by a factor of 1.0165, corresponding to the ratio between the experimentally found pK_a of phenol (9.88) and the calculated one (9.72). All calculations were performed using the B3LYP/6-311+G(d,p) level of theory. Solvent effects were considered through the continuum SMD model of water [32]. Besides this, the program Marvin (Marvin 20.8.0, 2020, ChemAxon, http://www.chemaxon.com) from the software package ChemAxon, which uses quantitative structure property relationships (QSPRs) based on various chemical descriptors and is fragment-based, was used for comparison.

2.4. (Photo)stability measurement

To evaluate the stability/photostability of the studied compounds, stock solutions in DMSO were diluted in a mixture of phosphate buffers (50 mM, pH 7.4) with methanol (2:1, *v:v*). The final concentration of compounds was 20 μM and of DMSO 2% (*v/v*). Immediately after the

preparation of cannabinoid solution, the spectrum scan was done using an UV-VIS spectrophotometer (UV–2401PC; Shimadzu, Japan) with a wavelength range of 250–450 nm in a quartz cuvette with a 1-cm path length. To determine the effect of oxygen on the (photo)stability of cannabinoids, solutions of the tested compounds were divided into four aliquots immediately after their preparation and sealed in plastic flasks with a plugged cap. Two flasks were bubbled with argon (conditions without oxygen).

Two flasks (with and without oxygen) were exposed to UVA radiation (20 J/cm^2). A SOL 500 solar simulator equipped with a H1 filter transmitting at wavelengths of 320–400 nm was used as the source of UVA light. The UVA output was measured with an UVA-meter (Dr. Hönle UV Technology, Germany). During the irradiation, the flasks were placed on ice-cold panels to eliminate heating of the solution and possible thermal decomposition. In parallel during the irradiation, two flasks (with and without oxygen) were incubated in the dark. Immediately and 24 h after UVA irradiation, the absorption spectrum was scanned using an UV-VIS spectrophotometer in the same way as samples without UVA irradiation in the presence or absence of oxygen. In parallel with the spectral evaluation, electrochemical analyses of samples (sec. 2.2.) and LC-MS analysis (sec. 2.6.) were performed.

2.5. Toxicity, phototoxicity and photoprotection

2.5.1. Cell cultures

Normal human dermal fibroblasts (NHDF) were obtained from the skin fragments of medically healthy adult donors. The tissue specimens were obtained from patients undergoing plastic surgery at the Department of Plastic and Aesthetic Surgery (University Hospital, Olomouc). The use of skin tissue complied with the Ethics Committee of the University Hospital in Olomouc and Faculty of Medicine and Dentistry, Palacky University, Olomouc (date: 6.4.2009, ref. number: 41/09). All patients had given their written informed consent. The skin fragments and NHDF were cultured as described earlier [33]. NHDF were used between the 2nd and 4th passage. For experiments, cells were seeded on 96-well collagen-coated plates at a density of 0.5×10^5 cells per cm^2. Experiments were performed in four independent repetitions with the use of cells from four donors to minimize the individual sensitivity of donor cells.

A spontaneously transformed aneuploid immortalized human keratinocyte cell line (HaCaT) was obtained from CLS (Eppeheim, Germany). HaCaT was grown in culture medium consisting of Dulbecco's Modified Eagle Medium (DMEM) supplemented with fetal calf serum (10%, *v/v*), penicillin (100 mg/mL) and streptomycin (100 U/mL). For experiments, cells (between the 50th and 60th passage) were seeded on 96-well plates at a density of 1.0×10^5 cells per cm^2. Experiments were performed in four independent repetitions.

2.5.2. Cytotoxicity of test compounds

NHDF or HaCaT were treated with CBD, CBC, CBG and CBN (0.78–100 μmol/L) and with DMSO (0.5%, *v/v*) in serum-free DMEM for 24 h. Control cells were treated with serum-free medium containing DMSO (0.5%, *v/v*) under the same conditions. After 24 h (37 °C, 5% CO_2), cell damage was evaluated by NR incorporation into viable cells [34]. Medium was discarded and NR solution (0.03%, *w/v*, PBS) was applied. After 60 min, the NR solution was discarded, cells were fixed with a mixture of formaldehyde (0.5%, *v/v*) and $CaCl_2$ (1%, *w/v*) in a 1:1 ratio, and then NR was dissolved in methanol (50%, *v/v*) with acetic acid (1%, *v/v*). After 5 min of intensive shaking, absorbance was measured at 540 nm.

2.5.3. Phototoxicity of tested compounds

Two plates with NHDF or HaCaT were pre-treated with CBD, CBC, CBG and CBN (0.78–100 μmol/L) and with DMSO (0.5%, *v/v*) in serum-free DMEM for 1 h. Control cells were treated with serum-free medium containing DMSO (0.5%, *v/v*) under the same conditions. After incubation, cells were washed twice with PBS and then PBS supplemented with glucose (PBS-G; 1 mg/mL) was applied. Randomly, one plate was then exposed to a non-cytotoxic dose of UVA radiation (5.0 J/cm^2 for NHDF and 7.5 J/cm^2 for HaCaT) using a SOL 500 solar simulator (Dr. Hoenle Technology, Germany) equipped with an H1 filter transmitting at wavelengths of 320–400 nm. The intensity of UVA radiation was evaluated before each irradiation with a UVA-meter (Dr. Hoenle Technology, Germany). During irradiation, the plate was incubated on a cold panel to limit overheating. The second (non-irradiated) plate was incubated in the dark for the period of irradiation. After UVA exposure, PBS-G was discarded and serum-free medium was applied. After 24 h (37 °C, 5% CO_2), cell damage was evaluated by NR incorporation into viable cells. The phototoxic effect was evaluated as the % of viability of control cells.

2.5.4. UVA and UVB photoprotection potential of test compounds

Two plates with NHDF or HaCaT were pre-treated with CBD, CBC, CBG and CBN (0.78–6.25 μmol/L) and with DMSO (0.5%, *v/v*) in serum-free DMEM for 1 h. Control cells were treated with serum-free medium containing DMSO (0.5%, *v/v*) under the same conditions. After incubation, cells were washed twice with PBS and then PBS supplemented with glucose (1 mg/ml) was applied. Randomly, one plate was then exposed to a cytotoxic dose of UVA radiation (7.5 J/cm^2 for NHDF and 10.0 J/cm^2 for HaCaT) using a SOL 500 solar simulator (Dr. Hoenle Technology, Germany) equipped with a H1 filter transmitting at wavelengths of 320–400 nm. During irradiation, the plate was incubated on a cold panel to limit overheating. The second (non-irradiated) plate was incubated in the dark for the period of irradiation. After irradiation, serum-free DMEM was applied to both cells (irradiated and non-irradiated), and cells were then incubated for 24 h (37 °C, 5% CO_2).

To study the photoprotective effect against UVB, the plate was exposed to a cytotoxic dose of UVB radiation (150 mJ/cm^2) using the solar simulator equipped with a H2 filter transmitting at wavelengths of 295–320 nm. The other manipulations with cells were the same. The intensity of UVA or UVB radiation was evaluated before each irradiation with a UVA- or UVB-meter (Dr. Hoenle Technology, Germany). Cell damage was evaluated by NR incorporation into viable cells according to the following equation:

$$\text{Protection}\ (\%) = 100 - \left|\frac{As - Anc}{Apc - Anc}\right| \cdot 100$$

As … absorbance of sample (cells pre-incubated with test compounds in serum-free medium and irradiated)

Anc … absorbance of negative control (cells pre-incubated with DMSO in serum-free medium and non-irradiated, i.e. incubated in the dark)

Apc … absorbance of positive control (cells pre-incubated with DMSO in serum free medium and irradiated).

2.6. LC-MS method

UHPLC/MS analyses were performed in an ACQUITY I-Class UPLC system (Waters, Milford, MA, USA) equipped with a binary solvent manager, sample manager and column manager. Kinetex Polar C18 (100 × 2.1 mm, i.d. 2.6 μm; Phenomenex, CA, USA) was chosen as the analytical column. The system was set for binary gradient elution at a flow rate of 0.6 mL/min and a temperature of 25 °C. Mobile phase A consisted of 0.1% formic acid in water, mobile phase B was 0.1% formic acid in acetonitrile. The gradient profile started at: 0–11 min 50–70% B, 11–12.5 min 70–100% B, 12.5–13 min 100-50% B, 13–16 min 50% B. The injection volume was 2 μL.

The method development took place in a Xevo TQ-S mass spectrometer (Waters), a triple quadrupole mass spectrometer with ESI ion source operated in positive mode. Multiple reaction monitoring (MRM)

transitions were adapted from Ref. [35]. The capillary voltage was set to 3.0 kV and the sampling cone 30 V. The source temperature and the desolvation temperature were set to 120 °C and 320 °C, respectively. The cone and desolvation gas flows were 150 L/h and 900 L/h, respectively.

For analysis of oxidation products, a high-resolution Synapt G2-S Mass Spectrometer (Waters Corp., Manchester, UK) was connected to the UPLC system *via* an electrospray ionization (ESI) interface. The conditions were adapted from the Xevo TQ-S method. The ion source operated in positive ionization mode with a capillary voltage of 3.0 kV and a sampling cone at 30 V. The source temperature and the desolvation temperature were set to 120 °C and 320 °C, respectively. The cone and desolvation gas flows were 150 L/h and 900 L/h, respectively. The data acquisition range was from 50 to 1200 Da with a scan time of

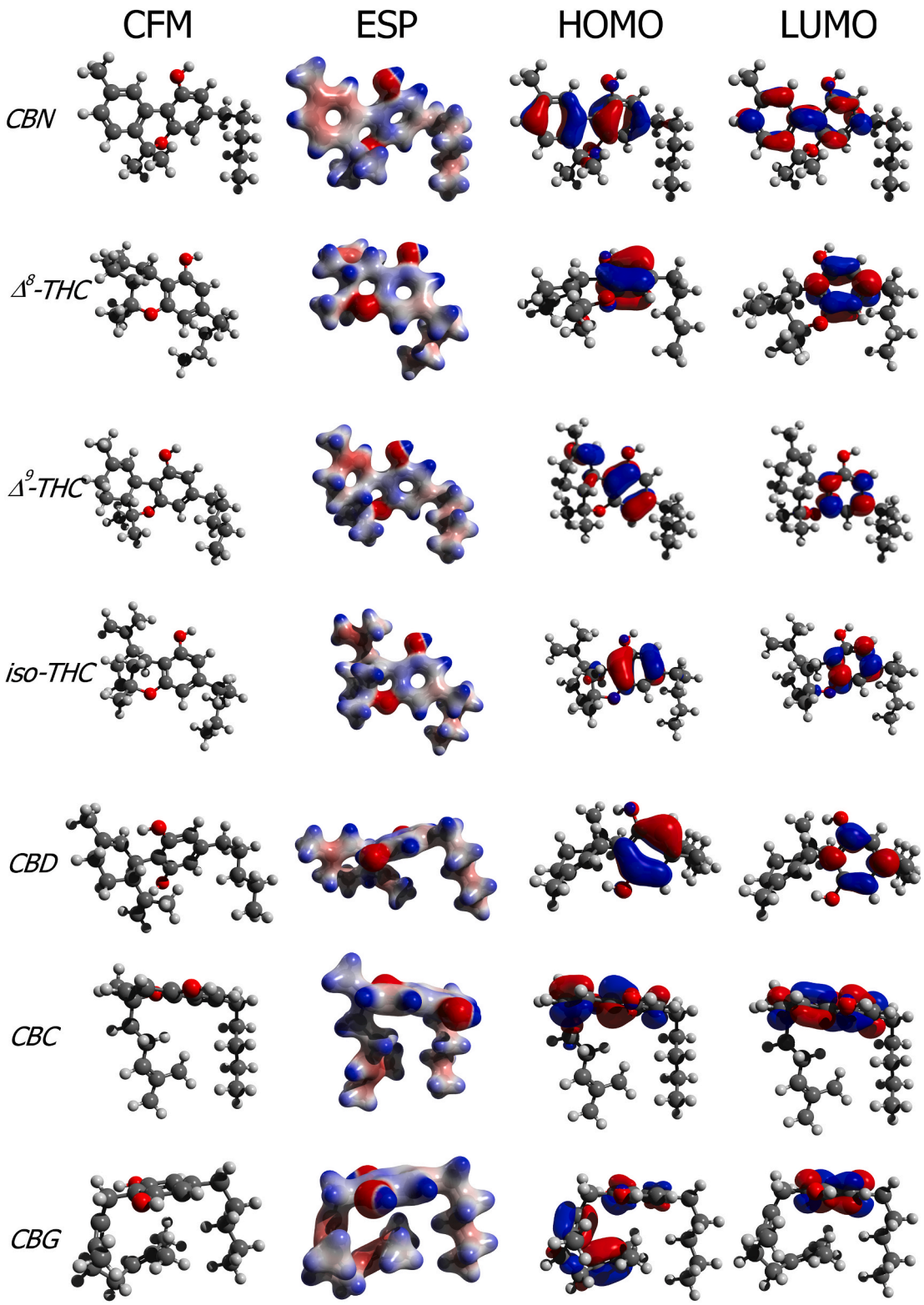

Fig. 1. The most stable conformer (CFM) with electrostatic potential (ESP) and HOMO/LUMO distributions of each of the studied cannabinoids.

0.2 s in MS^E mode (scan functions enabling the simultaneous acquisition of low-collision-energy (2 eV) and high-collision-energy (15–30 eV) mass spectra in a single experiment).

The instrument was calibrated using adducts of sodium formate in acetonitrile, and the corrections for accurate mass measurement were achieved using an external reference Leucine-enkephalin (20 μg/L in mixture of water:acetonitrile:formic acid (100:100:0.2), flow rate of 5 μL/min). The LC-MS system was controlled with MassLynx V4.1 (Waters), and the post-acquisition processing of the data was performed using the MetaboLynx XS Application Manager (Waters). Concerning the accurate mass measurement, MS data outlying the range of ±5 ppm were not considered.

3. Results and discussion

Here, we focused on the complex investigation of cannabidiol (CBD), cannabigerol (CBG), cannabinol (CBN), cannabichromene (CBC), Δ^8-tetrahydrocannabinol (Δ^8-THC), Δ^9-tetrahydrocannabinol (Δ^9-THC), and iso-Δ^8-tetrahydrocannabinol (iso-THC), see Scheme 1. The conformational variability, electronic structures, electron-donor and acido-basic properties were studied using voltammetric and DFT calculation approaches. The stability profiles of the phytocannabinoids based on their ability to be oxidized is described together with the photo-degradation processes by using voltammetry, UV-VIS spectrophotometry and liquid chromatography-mass spectrometry (LC-MS). Finally, the cytotoxicity and protective properties of CBD, CBC, CBG and CBN were tested using UVA- and UVB-irradiated spontaneously immortalized human keratinocyte cell line (HaCaT) and normal human dermal fibroblasts (NHDF).

3.1. Conformational variability and electronic structure

The potential energy surface scan of investigated cannabinoids shows that, unlike the rigid cyclic part of the molecule, the aliphatic side chains of these molecules are very flexible and there are a large number of conformers that only differ in energy by a tiny amount. This means that besides the structure of the global minimum, several other geometries of the given compound will be non-negligibly populated at room temperature. The most stable conformers are those where a favorable C–H ...π interaction appears, which is clearly visible in the structure of the global minimum of CBG, where a strong interaction between the terpene side chain and aromatic ring occurs. Whereas in the study [36] the authors considered the conformers containing aliphatic side chains in an *all-trans* position, we found that those are typically less stable by 3–12 kJ/mol than the global minimum. It means that they do not appear among the geometries of the ten most stable conformers listed in Supplementary Information.

The DFT computational approach shows that for all the studied compounds, the HOMOs and LUMOs correspond to the π and π* orbitals of the benzene ring (Fig. 1). The delocalization of these orbitals is often expanded over neighboring parts of the compound containing double bonds. The HOMO energy values of all compounds can be found in a narrow range of 0.3 eV around −8 eV (see Table 1 and Supplementary Information), in agreement with previously published data [37,38] and independently of the type of solvent used. Molecular electrostatic potential (ESP) surfaces of cannabinoids can be found in Fig. 1. All oxygen atoms possess a negative potential (red) both in aromatic phenol as well as in ether groups. An excess of negative charge can also be found on carbon atoms participating in isolated double bonds and carbon atoms of the phenyl ring of CBN. Positive potential (blue) is found on all hydrogen atoms, especially in the phenol ring.

3.2. Redox behavior – oxidative transformation and acido-basic properties

Oxidation of the cannabinoids was investigated using SWV at a GCE. At pH 7.4, all test substances undergo an electrochemical transformation around the potential E_p +0.5 V *vs.* Ag/AgCl/3 M KCl (Fig. 2). Based on previously published results, we can designate the investigated molecules as moderately-effective electron-donors, *i.e.* substances with a slight reducing potential. Electrochemical analyses confirmed previously published results on the antiradical and antioxidant properties of cannabinoids. An example is a robust study in which the authors monitored the antiradical capacity of Δ^9-THC, CBD and *C. sativa* extracts using spectrophotometric as well as electrochemical methods [39]. The results indicate that it is highly dependent on the experimental conditions and the method chosen. If, for example, CBD is studied in an oil environment, it may also have a higher antioxidant potential than

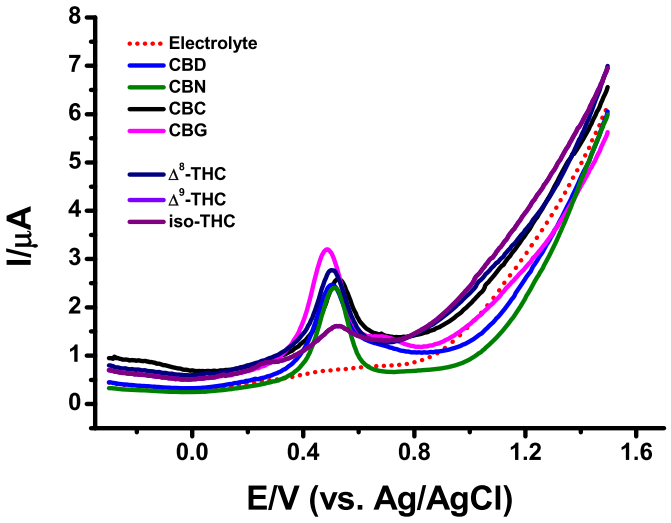

Fig. 2. Square-wave voltammograms of cannabinoids in Britton-Robinson buffer at pH 7. The analyzed compound (20 μM) was accumulated at open circuit potential for 60 s prior to each analysis. The oxygen was removed from the supporting electrolyte with an argon stream. The SW voltammetric scan was performed from −0.3 to +1.5 V at a frequency of 200 Hz. SWV records for alkaline and acidic pH can be found in Supplementary Information.

Table 1
HOMO-LUMO characteristics and HOMO-LUMO gap (all in eV) of the most stable conformer of the studied cannabinoids in different solvents. All calculations were performed at the wB97XD/6-311++G(d, p) level of theory.

Solvent	Water			Methanol			Octanol		
Compound	HOMO	LUMO	LUMO-HOMO	HOMO	LUMO	LUMO-HOMO	HOMO	LUMO	LUMO-HOMO
CBC	−7.768	0.704	8.472	−7.842	0.687	8.529	−7.711	0.807	8.518
CBD	−8.160	1.070	9.230	−8.139	1.047	9.186	−7.942	1.018	8.960
CBG	−8.159	1.056	9.215	−8.168	1.072	9.240	−8.089	1.012	9.101
CBN	−7.858	0.556	8.414	−7.844	0.566	8.410	−7.686	0.727	8.413
Δ^8-THC	−7.988	1.032	9.020	−7.972	1.029	9.001	−7.825	1.011	8.836
Δ^9-THC	−8.083	1.045	9.128	−8.072	1.070	9.142	−7.910	1.048	8.958
iso-THC	−8.045	1.045	9.090	−8.055	1.072	9.127	−7.925	1.045	8.970

α-tocopherol [40]. From the point of view of electrochemical analysis, the oxidation of highly effective low-molecular weight antioxidants usually occurs at *E*p lower than +0.2 V (*vs*. Ag/AgCl/3 M KCl). This was recently demonstrated for selected vitamins, their conjugates and trolox, under identical experimental conditions as in this study [41]. The OH group or groups occurring on the benzene skeleton of the investigated molecules participate in the anodic reaction (Scheme 1). With Δ^9-THC, -1 e^-/-1 H^+ oxidation to form a quinone product was described [42].

The oxidation of cannabinoids is associated, similarly to other phenolic compounds, with the formation of radical forms, which leads to the formation of passivating oligo- or polymeric structures on the electrode surface [43]. The anodic reaction is accompanied by adsorption phenomena in the aqueous medium. This can be used for the adsorptive accumulation of the cannabinoids on the electrode surface before the measurement. Cannabinoids are lipophilic molecules, and this facilitates their interaction with electrode materials or materials designed to preconcentrate them [44,45].

In this study, SWV experiments were performed at pH 4, 7.4 and 9 (Fig. 2 and Figs. S1-S2 in Supplementary Information). The electrochemical conversion of cannabinoids is a pH-dependent process, where with increasing pH there is a shift in E_p towards less positive potentials, see Table 2 and Fig. S3 in Supplementary Information. In an alkaline environment, an accelerated degradation of cannabinoids as well as other phenolic derivatives can occur in the presence of oxygen. This is related to the deprotonation of the investigated molecules. With cannabinoids, they are only deprotonated in the pH range of 9–10. At physiological pH, cannabinoids are practically in a protonated state, which prevents their oxidative degradation (more about the degradation of cannabinoids below). The calculated *p*Ka values for all studied cannabinoids are given in Table 3. The program Marvin predicts the pK_a values of cannabinoids in very narrow range of 0.1, treating the cannabinoids as slightly stronger acids than phenol. The *ab initio* pK_a values are distributed across a larger interval between 9.7-10.8, determining the cannabinoids to be either comparable (CBG, CBN) or slightly weaker acids than phenol. Such values agree well with experimentally found ones published in Ref. [46].

For a more detailed (mechanistic) insight into the reactivity and oxidative transformations of cannabinoids, we used DFT computational approaches (Fig. 1). Electron abstraction during cannabinoid oxidation corresponds to the distribution of HOMO and its energy levels, which in the aqueous environment range between −7 and −8 eV (Table 1) and not only correspond to the measured oxidation potentials (Table 2), but also to the ionization potentials (Tab. S1 in Supplementary Information) of the investigated molecules. The relative small HOMO-LUMO gaps and the lowest ionization potentials were observed for CBN and CBC. In addition to the fact that the above-mentioned methods allow us to quantify the electron-donor capacity of cannabinoids, primarily electrochemical SWV analysis can also be used to evaluate their oxidative stability. The oxidative stability of cannabinoids could be an important parameter for the development of new cannabinoid preparations. This will be discussed in the following section.

Table 2
Oxidation potentials (E_p values) for cannabinoids analyzed by SWV in Britton-Robinson buffer of different pH levels (vs. Ag/AgCl/3 M KCl). For other details, see Fig. 2.

Compound	pH 4	pH 7.4	pH 9
CBC	0.708	0.524	0.432
CBD	0.701	0.506	0.403
CBG	0.673	0.492	0.390
CBN	0.717	0.511	0.425
Δ^8-THC	0.721	0.511	0.415
Δ^9-THC	0.698	0.516	0.421
iso-THC	0.716	0.547	0.431

Table 3
pK_a values for different cannabinoids calculated with program Marvin and based on *ab initio* approach.

Compound	Marvin	*Ab initio*
CBC	9.47	10.26
CBD	9.43	10.32
CBG	9.46	9.82
CBN	9.32	9.73
Δ^8-THC	9.32	10.48
Δ^9-THC	9.34	10.51
iso-THC	9.86	10.84

3.3. Stability and photodegradation processes

Stability data related to the long-term storage of medical cannabis, the decomposition of cannabis oils and pharmaceuticals in solid form can be found in the literature, see the stability of dronabinol capsules [47]. Stability data are also available for the purposes of forensic analysis [48]. In terms of basic research and biochemical studies, no comprehensive comparative study on the stability and reactivity of cannabinoids has been published yet. In this study, we focus on the

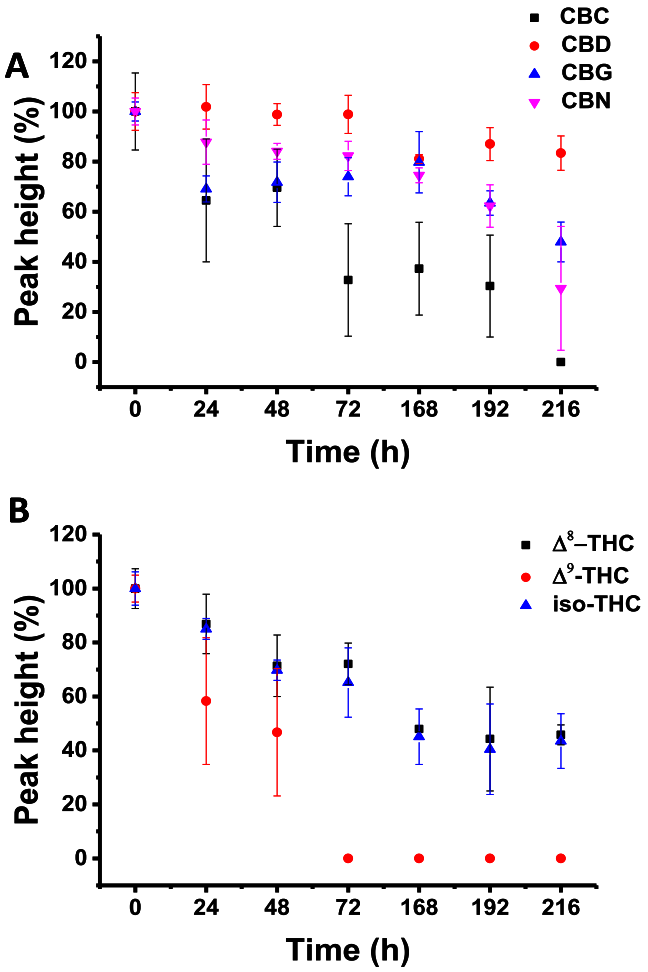

Fig. 3. Stability of cannabinoids (20 μM) based on measurement of SWV oxidation peak height over time. The stability evaluation for non-psychotropic cannabinoids and THC isomers are shown in panels **A** and **B** ($n = 3$). Both the incubation step and SWV analysis were performed in 0.1 M phosphate buffer (pH 7.4) with methanol (2:1, *v/v*). Prior to each analysis, the analyzed compound was accumulated at open circuit potential for 60 s. The oxygen was removed from the supporting electrolyte with an argon stream. The SW voltammetric scan direction was as follows: from −0.3 to +1.5 V. A frequency of 200 Hz was used.

stability and photostability of cannabinoids at pH 7.4 in an aqueous environment. The results obtained by SWV measurements are shown in Fig. 3. In these experiments, a decrease in the oxidation peaks (Fig. 2) of cannabinoids was observed, the decrease of which generally indicates oxidative degradation of the investigated substances.

For non-psychotropic cannabinoids, the stability study was performed at pH 7.4 for 216 h, in the dark, at room temperature and in the presence of molecular (atmospheric) oxygen. Oxidation stability decreases in the following order: CBD > CBG ≥ CBN > CBC (Fig. 3A). The reduced stability for CBN and CBC corresponds well with lower HOMO energy levels and ionization potentials (Tabs. 1 and S1 in Supplementary Information), which are closely related to the electron-donor capacity of the investigated cannabinoids. Furthermore, the results are consistent with a lower stability of CBC in a slightly acidic environment, where [4+2] cycloaddition occurs to form cannabicitran [49]. The substances are stable within 1 h, then there is a gradual decrease in the height of oxidation SWV peaks depending on the kinetics of decomposition (oxidation) of the examined samples. These measurements are based on the assumption that if the OH groups of cannabinoids are oxidized during the stability study, they can no longer be further oxidized in the electrochemical experiment. After 24 hours, there was a 20–40% decrease in the oxidation peaks of non-psychotropic cannabinoids. The stability of the Δ^8-THC and iso-THC was observed under the same experimental conditions, and was comparable to the stability of CBG and CBN (Fig. 3B). Unlike other cannabinoids, the Δ^9- THC was significantly less stable, and its degradation after 24 h corresponded to approx. 50%. After three days of incubation, Δ^9-THC could no longer be detected.

In further experiments, we focused on a study of the photodegradation of non-psychotropic cannabinoids (Fig. 4). Analyses were performed under the same conditions as for the long-term stability study (Fig. 3), only the sample was irradiated with UVA at the beginning of the stability experiment with a single dose of 20 J/cm^2. The sample was analyzed immediately after irradiation (0 h), and also 24 h after the irradiation, when it was stored in the dark. SWV analysis showed that the CBD and CBG samples were stable under the chosen experimental procedure. Moderate photodegradation was observed in CBN and CBC (Fig. 4). CBC is known to be photochemically unstable and undergoes [2+2] photocycloaddition to form cannabicyclol [50]. However, when interpreting the results, we must assume that the SWV analysis corresponds to oxidative degradation and is not an absolute method, mainly due to the fact that some photodegradation products may also be electroactive or undergo interfering adsorption processes. For this reason, we applied other methods such as UV-VIS spectrophotometry and LC-MS analysis. The UV-VIS spectra of the tested substances are shown in Fig. 5A. Well-developed spectra can only be obtained for CBC and CBN. Thus, after irradiation, decreases in the absorbance of both substances at 280 nm, which is related to the presence of double bonds, were investigated. Concretely, 10–20% decreases in the absorbance of CBC and CBN were observed in the irradiated samples (Fig. 5B and C) in accordance with the electrochemical analysis (Fig. 4A,D). The LC-MS method was also used to confirm the photodegradation after 24 h, where the chromatographic peak of the respective substances was monitored, for details see Figs. S4 and S5 (Supplementary Information). The results show increased degradation for CBC and CBN consistent with the electrochemical and UV-VIS spectral analyses (Fig. 5D). In general CBD, which is most commonly used in cosmetics and other topical pharmaceuticals today, exhibits good stability, whether or not it has been irradiated with UVA radiation. The stability of all substances was

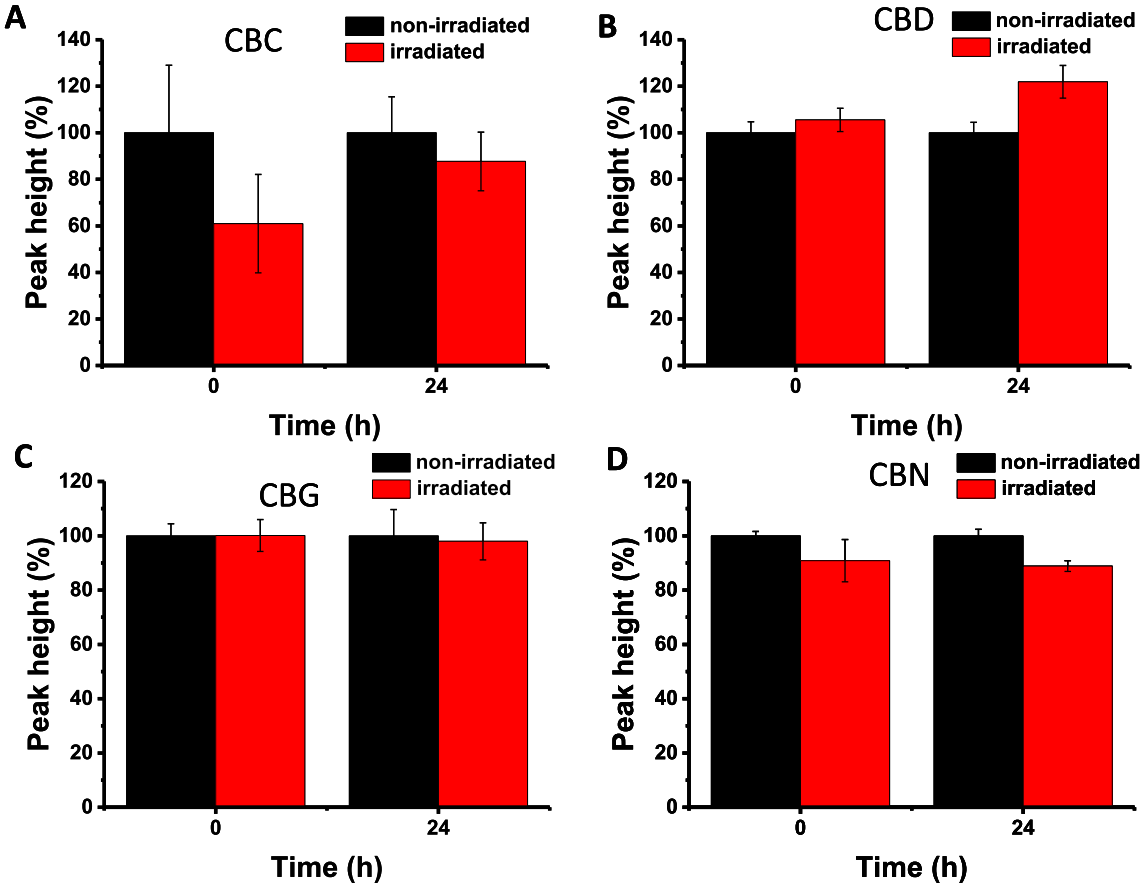

Fig. 4. Changes in SWV oxidation peaks of CBC **(A)**, CBD **(B)**, CBG **(C)** and CBN **(D)** after UVA irradiation ($n = 3$). The cannabinoids (20 μM) were dissolved in 0.1 M phosphate buffer (pH 7.4) with methanol (2:1, *v/v*). The samples were analyzed by SWV immediately (0 h) and 24 h after UVA irradiation (20 J/cm^2). The samples were incubated in the dark at room temperature in the presence of atmospheric oxygen. For more details on SWV, see Fig. 3.

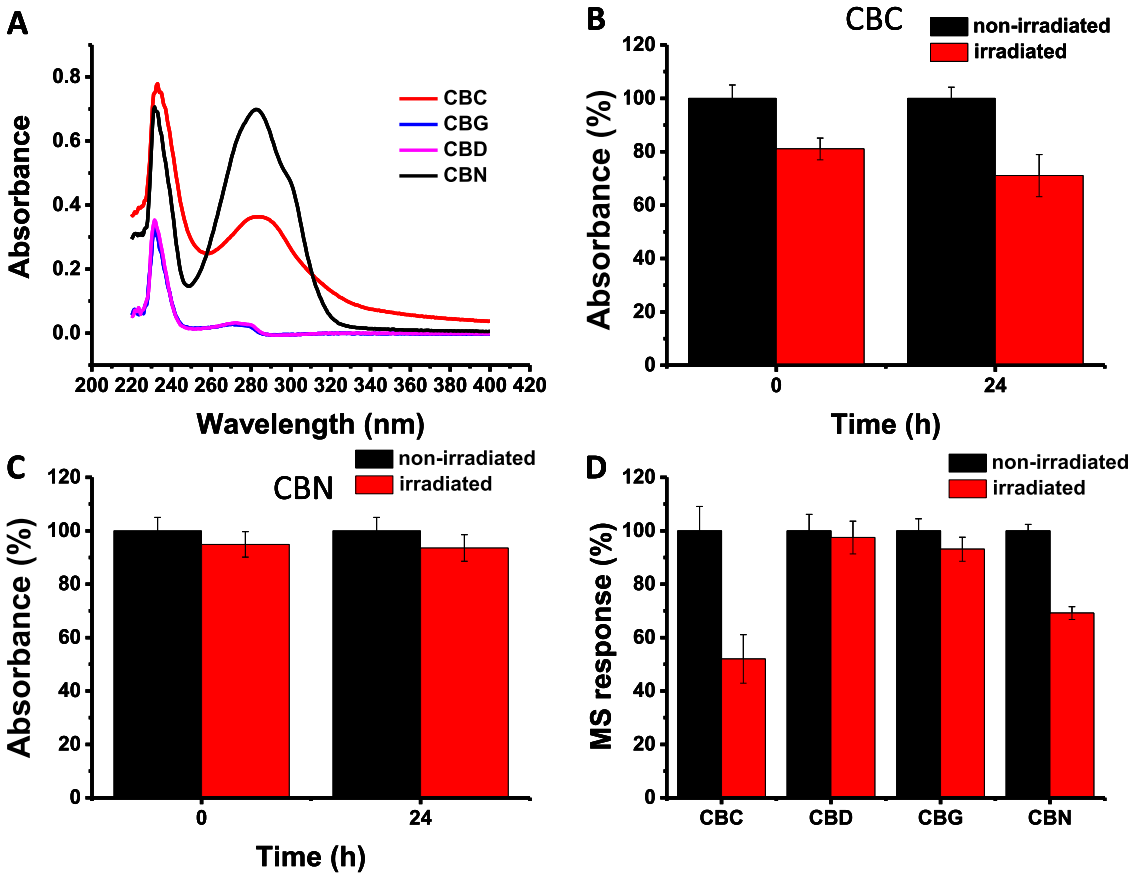

Fig. 5. UV-VIS spectra of cannabinoids (50 μM) in 0.1 M phosphate buffer (pH 7.4) with methanol (2:1, *v/v*) (**A**). UVA-photostabilty of 20 μM CBC **(B)** and CBN **(C)** expressed as % of absorbance changes at 280 nm immediately and 24 hours after UVA irradiation. **(D)** UVA-photostability of cannabinoids (20 μM) measured as total ion current MS response after 24 h of incubation. The incubation of samples was done in the dark at room temperature and in the presence of atmospheric oxygen (n = 3, for panels **B**–**D**).

investigated under ambient conditions in the presence of atmospheric oxygen. If oxygen is displaced from the solution, some degradation processes can be significantly suppressed, which corresponds to analyses of other hydroxy-substituted aromatic compounds [51].

3.4. Cytoprotective effects under UV irradiation

Based on the spectra of the individual cannabinoids (Fig. 5A), it is clear that CBN and CBC could have a (direct) protective effect against irradiation in the UVB region, in contrast to CBG and CBD, which do not absorb at the corresponding wavelengths. Although CBG and CBD do not show the typical spectrum, they were also included in the testing, because both cannabinoids can be used in dermal applications. Firstly, the toxicity and phototoxicity of the cannabinoids (0.78–100 μM) were assessed on dermal cells on primary human dermal fibroblasts (NHDF) and a cell line of human keratinocytes (HaCaT). HaCaT were used instead of primary keratinocytes in the pilot screening for phototoxic and/or photoprotective properties. The toxicity was dose dependent and was expressed as the half-maximal cytotoxic concentration IC_{50} (μM), see Table 4. NHDF were more sensitive than HaCaT. The same concentration range (0.78–100 μM) was used for evaluating the phototoxic potential of the tested compounds. As shown Table 5, the non-toxic dose of UVA radiation did not accelerate the toxicity of the parent compounds. These results show that the studied compounds have no phototoxic potential. The higher values of IC_{50} (lower toxic effect) found in the phototoxic experiment is associated with a 1-h treatment with the studied compounds compared to cytotoxicity testing (Table 4), which was evaluated after the 24-h treatment.

Based on the cytotoxicity findings, non-toxic concentrations of the studied compounds were used for the UVA- and UVB-photoprotective experiments (0.781–6.25 μM). For all the tested compounds, a higher viability (amount of incorporated NR) of UVA- or UVB-irradiated cells pre-treated with the studied cannabinoids was observed compared to non pre-treated ones (Fig. 6). In general, the tested compounds exhibited higher UVA and UVB protection of NHDF than of HaCaT. Our results

Table 4
Cytotoxicity (IC_{50} values; μM) of non-psychotropic cannabinoids on normal human dermal fibroblasts (NHDF) and human keratinocyte cell line (HaCaT), n = 4.

Compound	NHDF	HaCaT
CBN	7.15 ± 0.65	12.98 ± 1.35
CBC	4.73 ± 0.54	10.18 ± 1.03
CBG	5.88 ± 0.48	16.94 ± 1.74
CBD	7.15 ± 0.65	12.85 ± 1.17

Table 5
UVA phototoxicity (IC_{50} values; μM) of non-psychotropic cannabinoids on normal human dermal fibroblasts (NHDF) and human keratinocyte cell line (HaCaT), n = 4.

Compound	NHDF		HaCaT	
	non-irradiated	irradiated	non-irradiated	irradiated
CBN	14.64 ± 1.24	18.74 ± 1.24	12.07 ± 1.10	16.32 ± 1.23
CBC	20.75 ± 1.98	20.61 ± 1.55	20.74 ± 1.65	20.61 ± 1.45
CBG	21.23 ± 2.05	24.10 ± 2.25	16.21 ± 1.37	20.14 ± 1.99
CBD	12.97 ± 1.01	19.18 ± 1.47	10.74 ± 1.00	16.93 ± 1.36

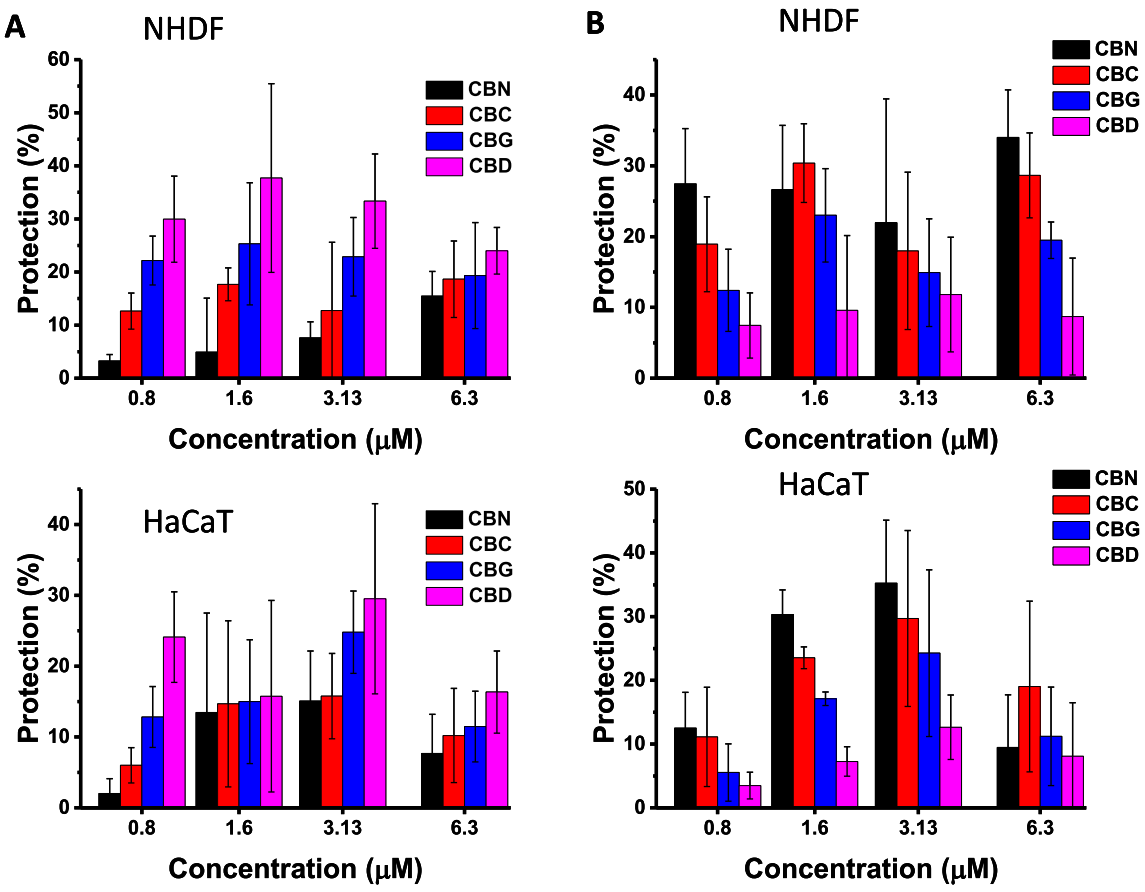

Fig. 6. UVA **(A)** and UVB **(B)** protectivity of non-psychotropic cannabinoids on normal human dermal fibroblasts (NHDF) and human keratinocytes (HaCaT), $n = 4$. For more details, see sec. 2.5.4.

demonstrate the photoprotective effects of other phytocannabinoids, with exception of CBD, on human skin fibroblasts and keratinocytes (HaCaT) over the entire solar region of UV radiation (UVA and UVB) for the first time.

3.5. Biological relevance of the results and discussion

The obtained physicochemical characteristics of the studied cannabinoids (sec. 3.1. and 3.2) are in good agreement with their stability and reactivity, regardless of whether the samples were UV-irradiated or not (sec. 3.3). The THC:CBD ratio plays a key role in practically used preparations [52]. However, their different degradation kinetics (Fig. 3) should be taken into account when interpreting experiments (but also clinical trials) where both THC and CBD are involved. Cannabinoids are also used in many topical preparations and their (photo)stability cannot be neglected, because the effects studied in the experiments may not be related to the biological effect of the parent cannabinoids, but to their degradation or biotransformation products. It has been shown that the biological activity of oxidized CBD may be different from the parent molecule [53], for example, the oxidation product of CBD inhibited topoisomerase II α and β, which was not observed for CBD itself. The degradation of cannabinoids is most likely based on oxidative transformation, which was confirmed electrochemically (Fig. 3). The reactivity of oxidation products (most probably quinones) should be investigated in further studies with a focus on other redox processes, including reductive transformations. The electrochemistry of Δ^9-THC metabolites can be found here [54], data on the other cannabinoids are not available. As for transformation to quinones, a CBG quinone derivative was identified in a structure-activity relationship study. For this derivative, oxidative modification of the resorcinol moiety has been shown to affect binding affinity to CB_1 and CB_2 receptors and PPARγ [55]. The selected quinone (VCE-003) was proposed as a candidate for anti-inflammatory effect testing [56]. The oxidation products of cannabinoids also show modulation of the activity of liver biotransformation enzymes [56]. More information on the stability of cannabinoids in selected formulations can be found in the following studies [57–59].

As for the antioxidant action of phytocannabinoids, they most likely interact directly with ROS or other reactive molecules to a limited extent. There is clear evidence that the endocannabinoid system affects the redox balance of cells [57–59]. The CB_1 and CB_2 receptors can be involved in the elimination but also in the production of free radicals, depending on intrinsic cell status and external stimuli. Most of the studies targeting redox balance and the endocannabinoid system are based on the application of CB_1 and/or CB_2 receptor agonists or antagonists *in vitro* after the application of toxic compounds (often oxidants) or induction of inflammation using a lipopolysaccharide-based approach [60]. In addition, CB_1 and CB_2 receptors and also other membrane receptors (PPARγ, TRP, GPR, serotonin ($5HT_{1A}$) and adenosine (A_{2A}) receptors) and channels are involved in redox homeostasis [16]. The mode of action involving the above-mentioned receptors is based on cannabinoid ligand binding, which results in the increase or decrease in the level of antioxidant or pro-oxidant enzymes. This mechanism is also called ‘indirect’ or receptor-driven. In addition to this, there is also the hypothesis that cannabinoids can act as ‘direct’ lipophilic radical scavenging species. The results presented here support this indirect mechanism of protection due to a moderate or relatively low electron-donor ability of phytocannabinoids in comparison to other (established) low-molecular radical scavengers or antioxidants [41, 61–63].

In the context of dermal cytoprotection (sec. 3.4) CBD induces the

synthesis of the cytoprotective enzyme heme oxygenase 1 (HMOX1) in keratinocytes in an Nrf2-independent manner. This was accompanied by an increase in nuclear export and proteasomal degradation of the Nrf2 transcriptional repressor Bach1, and the expression of cytokeratins 16 and 17 in keratinocytes [64]. The fact that CBD induced the expression of several Nrf2 target genes should be the main mechanism for its photoprotective action, and could be extrapolated to the biological activities of other studied phytocannabinoids. In addition, it was reported that CBD reduced the redox imbalance caused by exposure to UVB/hydrogen peroxide in keratinocytes, estimated by superoxide anion radical generation, total antioxidant status and consequently lipid peroxidation product(s) level [65]. The protective effect of CBD on viability of keratiocytes and melanocytes [66] and skin fibroblasts [67] following UV irradiation was also recently shown.

Also, CBD stimulated ROS generation in mitochondria that was accompanied by apoptosis in monocytes [68]. Antioxidant *vs*. pro-oxidant effects and their mutual balance or the localization of their action is in accordance with the pleiotropic action of cannabinoids. However, we should always perceive the pleiotropic effects of cannabinoids with regard to the fact that the primary molecular targets are CB_1 and/or CB_2 and other receptors. The interaction with other cellular components will depend on the cell type and the concentration of applied cannabinoids, etc. This is in accordance with the biphasic effect of phytocannabinoids and the phenomena that we refer to in the literature as entourage effects. Phytocannabinoids are redox-active molecules, and also their interaction with other redox-active ligands (or transition metals) is one of the possible mechanisms of action that should be considered [69].

In summary, phytocannabinoids are relatively weak or moderate electron donors, and therefore may be involved to a limited extent in the 'direct' scavenging of free radicals and the elimination of oxidizing agents. However, their action as low-molecular weight antioxidants is significantly limited by their relatively low bioavailability and strictly dependent on the environment in which they act, *e.g.* the cytoplasm *vs*. cell membranes. Based on the available data, we conclude that the antioxidant or (photo)/cytoprotective action of phytocannabinoids will primarily occur 'indirectly' by their interaction with specific receptors and the activation of stress (redox-sensitive) protection signalling pathways (the Nrf2 pathway). For a more detailed understanding of the *in vivo* antiradical and antioxidant properties of phytocannabinoids, it will be necessary to conduct more extensive research focused mainly on the 'direct'/'indirect' antioxidant effect of cannabinoids in skin, but also in the GIT. In any case, the designation of cannabinoids as 'effective low-molecular weight antioxidants' should not be overused. Instead, we should think about phytocannabinoids as 'redox-active modulators of homeostatic mechanisms of the cell'.

4. Conclusions

Despite the fact that phytocannabinoids contain hydroxyl groups bound to double-bonded carbons, they are compounds which are relatively stable under ambient conditions at pH 7.4 in an aqueous medium. CBD exhibits the highest stability, CBG, CBN and CBC are less stable. The degradation of these non-psychotropic phytocannabinoids is very slow in an aqueous medium, and thus does not distort short-term experiments on the order of hours. In long-term experiments, it is necessary to take into account the degradation kinetics of individual substances. As for the two phytocannabinoids that are the most pharmacologically active and most used in practice, psychotropic Δ^9-THC degrades approximately one order of magnitude faster than CBD. The high stability of phytocannabinoids is associated with the fact that their molecules are fully protonated at pH 7.4 (p*K*a for the investigated cannabinoids is ≥ 9).

Phytocannabinoids, especially CBD, are now massively applied in topical form as cosmetics or selected medical devices. Also for this reason, we investigated the photostability properties of non-psychotropic CBD, CBG, CBN and CBC. The degradation of CBN and CBC is shown to be accelerated after exposure to UVA radiation, with CBD (or CBG) being highly stable in the 24 h experiment. To gain a more complete view of phytocannabinoids and their topical applications, we paid attention to an *in vitro* study of their cytotoxic, phototoxic and photoprotective effects. Primary cultures of human skin fibroblasts and the keratinocyte cell line were used for this purpose. NHDF are approximately twice as sensitive to cannabinoids as HaCaT. Specifically, IC_{50} values for CBD after 24 h of incubation are 7.1 and 12.8 μM for NHDF and HaCaT, respectively. Phototoxicity of cannabinoids was excluded in both fibroblasts and keratinocytes. Extensive testing has shown that CBD is the most effective cytoprotectant after the UVA irradiation of skin cells. As for UVB photoprotective effects, CBN was the most effective.

Author statement

J.Va. performed electrochemical experiments, J.Vo. and D.S. performed *in vitro* cell experiments, M.Ka. designed and performed DFT calculations, M.Ko. and J.S. purified and synthesized phytocannabinoids, and J.Va., M.K. and J.Vo. wrote the paper.

Declaration of competing interest

J.S. has financial interest in CB21 Pharma Ltd., CBDepot Ltd. and PharmaCan Ltd. J.V. is a president of the scientific board of CB21 Pharma Ltd. All other authors declare that they have no conflicts of interest with the contents of this article.

Acknowledgements

The authors gratefully acknowledge the financial support of UPOL, RVO 61989592 and internal grant IGA_LF_2020_022, from the Ministry of Education, Youth and Sports. Synthetic work was supported by the project OP EIC Operational Programme (CZ.01.1.02/0.0/0.0/16_084/0010374). Computational resources were provided by CESNET LM2015042 and CERIT Scientific Cloud LM2015085, provided under the programme 'Projects of Large Research, Development, and Innovation Infrastructures'. The authors are indebted to Nina Kucharikova MSc (for *in vitro* cell experiments), Zita Skolarova DiS (for electrochemical analyses) and Ben Watson-Jones MEng (for linguistic assistance). We wish to thank Lumir O. Hanus DSc (Hebrew University of Jerusalem, Israel) for critical reading.

Appendix A. Supplementary data

Supplementary data to this article can be found online at https://doi.org/10.1016/j.freeradbiomed.2021.01.012.

References

[1] Y. Gaoni, R. Mechoulam, Isolation, structure, and partial synthesis of an active constituent of hashish, J. Am. Chem. Soc. 86 (1964) 1646–1647.
[2] F. Santavy, Notes on the structure of cannabidiol compounds, Acta Univ. Palacki. Olomuc. Fac. Med. 35 (1964) 5–9.
[3] R. Mechoulam, L.O. Hanus, R. Pertwee, A.C. Howlett, Early phytocannabinoid chemistry to endocannabinoids and beyond, Nat. Rev. Neurosci. 15 (2014) 757–764.
[4] A.A. Izzo, F. Borrelli, R. Capasso, V. Di Marzo, R. Mechoulam, Non-psychotropic plant cannabinoids: new therapeutic opportunities from an ancient herb, Trends Pharmacol. Sci. 30 (2009) 515–527.
[5] S. Pisanti, A.M. Malfitano, E. Ciaglia, A. Lamberti, R. Ranieri, G. Cuomo, M. Abate, G. Faggiana, M.C. Proto, D. Fiore, C. Laezza, M. Bifulco, Cannabidiol: state of the art and new challenges for therapeutic applications, Pharmacol. Ther. 175 (2017) 133–150.
[6] C.M. Andre, J.F. Hausman, G. Guerriero, *Cannabis sativa*: the plant of the thousand and one molecules, Front. Plant Sci. 7 (2016) 1–17.
[7] M.O. Bonn-Miller, C.V. Pollack Jr., D. Casarett, R. Dart, M. ElSohly, L. Good, M. Guzman, L.O. Hanus, K.P. Hill, M.A. Huestis, E. Marsh, S. Sisley, N. Skinner, J. Spahr, R. Vandrey, E. Viscusi, M.A. Ware, D. Abrams, Priority considerations for medicinal cannabis-related research, Cannab. Cannabinoid Res. 4 (2019) 139–157.

[8] A. Ligresti, L. De Petrocellis, V. Di Marzo, From phytocannabinoids to cannabinoid receptors and endocanabinoids: pleiotropic physiological and pathological roles through complex pharmacology, Physiol. Rev. 96 (2016) 1593–1659.

[9] D. Friedman, J.A. French, M. Maccarrone, Safety, efficacy, and mechanisms of action of cannabinoids in neurological disorders, Lancet Neurol. 18 (2019) 504–512.

[10] T.W. Klein, Cannabinoid-based drugs as anti-inflammatory therapeutics, Nat. Rev. Immunol. 5 (2005) 400–411.

[11] K.P. Hill, Medical marijuana for treatment of chronic pain and other medical and psychiatric problems A clinical review, JAMA, J. Am. Med. Assoc. 313 (2015) 2474–2483.

[12] G.W. Booz, Cannabidiol as an emergent therapeutic strategy for lessening the impact of inflammation on oxidative stress, Free Radic. Biol. Med. 51 (2011) 1054–1061.

[13] L.L. Yang, R. Rozenfeld, D.F. Wu, L.A. Devi, Z.F. Zhang, A. Cederbaum, Cannabidiol protects liver from binge alcohol-induced steatosis by mechanisms including inhibition of oxidative stress and increase in autophagy, Free Radic. Biol. Med. 68 (2014) 260–267.

[14] P. Mukhopadhyay, M. Rajesh, B. Horvath, S. Batkai, O. Park, G. Tanchian, R. Y. Gao, V. Patel, D.A. Wink, L. Liaudet, G. Hasko, R. Mechoulam, P. Pacher, Cannabidiol protects against hepatic ischemia/reperfusion injury by attenuating inflammatory signaling and response, oxidative/nitrative stress, and cell death, Free Radic. Biol. Med. 50 (2011) 1368–1381.

[15] B.M. Fonseca, M. Almada, M. Santos, H. Gaspar, F. Carvalho, N. Teixeira, G. Correia-da-Silva, Prooxidant effects of synthetic cannabinoids on endometrial cells, results in a strenous rebound adaptative effect, Free Radic. Biol. Med. 120 (2018). S134-S134.

[16] S. Atalay, I. Jarocka-karpowicz, E. Skrzydlewskas, Antioxidative and anti-inflammatory properties of cannabidiol, Antioxidants 9 (2020) 21.

[17] M.A. Elsohly, E.G. Boeren, C.E. Turner, Constituents of Cannabis sativa L. An improved method for the synthesis of dl-cannabichromene, J. Heterocycl. Chem. 15 (1978) 699–700.

[18] H.S. Yeom, H. Li, Y. Tang, R.P. Hsung, Total syntheses of cannabicyclol, clusiacyclol A and B, iso-eriobrucinol A and B, and eriobrucinol, Org. Lett. 15 (2013) 3130–3133.

[19] F. Pollastro, D. Caprioglio, P. Marotta, A.S. Moriello, L. De Petrocellis, O. Taglialatela-Scafati, G. Appendino, Iodine-Promoted aromatization of p -Menthane-Type phytocannabinoids, J. Nat. Prod. 81 (2018) 630–633.

[20] Y. Li, Y.J. Ding, J.Y. Wang, Y.M. Su, X.S. Wang, Pd-catalyzed C-H lactonization for expedient synthesis of biaryl lactones and total synthesis of cannabinol, Org. Lett. 15 (2013) 2574–2577.

[21] S. Kang, K. Davidsen, L. Gomez-Castillo, H. Jiang, X. Fu, Z. Li, Y. Liang, M. Jahn, M. Moussa, F. Dimaio, L. Gu, COMBINES-CID: an efficient method for de Novo engineering of highly specific chemically induced protein dimerization systems, J. Am. Chem. Soc. 141 (2019) 10948–10952.

[22] Y. Gaoni, R. Mechoulam, Hashish-VII, The isomerization of cannabidiol to tetrahydrocannabinols, Tetrahedron 22 (1966) 1481–1488.

[23] Y. Gaoni, R. Mechoulam, The ISO - tetrahydrocannabinols, Isr. J. Chem. 6 (1968) 679–690.

[24] L.J. Cheng, J.H. Xie, Y. Chen, L.X. Wang, Q.L. Zhou, Enantioselective total synthesis of (-)-delta-THC and (-)-delta-THC via catalytic asymmetric hydrogenation and S NAr cyclization, Org. Lett. 15 (2013) 764–767.

[25] M.A. Miteva, F. Guyon, P. Frog2 Tuffery, Efficient 3D conformation ensemble generator for small compounds, Nucleic Acids Res. 38 (2010) W622–W627.

[26] L. Goerigk, S. Grimme, A thorough benchmark of density functional methods for general main group thermochemistry, kinetics, and noncovalent interactions, Phys. Chem. Chem. Phys. 13 (2011) 6670–6688.

[27] M.D. Hanwell, D.E. Curtis, D.C. Lonie, T. Vandermeerschd, E. Zurek, G. R. Hutchison, Avogadro: an advanced semantic chemical editor, visualization, and analysis platform, J. Cheminf. 4 (2012).

[28] G. Scalmani, M.J. Frisch, Continuous surface charge polarizable continuum models of solvation. I. General formalism, J. Chem. Phys. 132 (2010) 114110.

[29] M.J. Frisch, G.W. Trucks, H.B. Schlegel, et al., Gaussian 16, Revision B.01, Gaussian, Inc., Wallingford CT, 2016.

[30] M.D. Liptak, G.C. Shields, Accurate pK_a calculations for carboxylic acids using Complete Basis Set and Gaussian-n models combined with CPCM continuum solvation methods, J. Am. Chem. Soc. 123 (2001) 7314–7319.

[31] J.R. Pliego, Thermodynamic cycles and the calculation of pK_a, Chem. Phys. Lett. 367 (2003) 145–149.

[32] A.V. Marenich, C.J. Cramer, D.G. Truhlar, Universal solvation model based on solute electron density and on a continuum model of the solvent defined by the bulk dielectric constant and atomic surface tensions, J. Phys. Chem. B 113 (2009) 6378–6396.

[33] A. Rajnochova-Svobodova, B. Zalesak, D. Biedermann, J. Ulrichova, J. Vostalova, Phototoxic potential of silymarin and its bioactive components, J. Photochem. Photobiol., B 156 (2016) 61–68.

[34] G. Repetto, A. del Peso, J.L. Zurita, Neutral red uptake assay for the estimation of cell viability/cytotoxicity, Nat. Protoc. 3 (2008) 1125–1131.

[35] T. Beres, L. Cernochova, S. Cavar Zeljkovic, S. Benicka, T. Gucky, M. Bercak, P. Tarkowski, Intralaboratory comparison of analytical methods for quantification of major phytocannabinoids, Anal. Bioanal. Chem. 411 (2019) 3069–3079.

[36] R.S. Borges, J. Batista, R.B. Viana, A.C. Baetas, E. Orestes, M.A. Andrade, K. M. Honorio, A.B.F. da Silva, Understanding the molecular aspects of tetrahydrocannabinol and cannabidiol as antioxidants, Molecules 18 (2013) 12663–12674.

[37] A. Kumer, N. Sarker, S. Paul, A. Zannat, The theoretical prediction of thermophysical properties, HOMO, LUMO, QSAR and biological indics of cannabinoids (CBD) and tetrahhdrocannabinol (THC) by computational chemistry, Adv. J. Chem. A 2 (2019) 190–202.

[38] M.N. Sarker, A. Kumer, M.J. Islam, S. Paul, A computational study of thermophysical, HOMO, LUMO, vibrational spectrum and UV-visible spectrum of cannabicyclol (CBL), and cannabigerol (CBG) using DFT, Asian J. Nanosci. Mater. 2 (2019) 439–447.

[39] A.C.M. Hacke, D. Lima, F. de Costa, K. Deshmukh, N. Li, A.M. Chow, J.A. Marques, R.P. Pereira, K. Kerman, Probing the antioxidant activity of delta-9-tetrahydrocannabinol and cannabidiol in *Cannabis sativa* extracts, Analyst 144 (2019) 4952–4961.

[40] Tura, M.; Mandrioli, M.; Toschi, T. G. Preliminary study: comparison of antioxidant activity of cannabidiol (CBD) and alpha-tocopherol added to refined olive and sunflower oils. Molecules 24; 2019.

[41] E. Vavrikova, V. Kren, L. Jezova-Kalachova, M. Biler, B. Chantemargue, M. Pyszkova, S. Riva, M. Kuzma, K. Valentova, J. Ulrichova, J. Vrba, P. Trouillas, J. Vacek, Novel flavonolignan hybrid antioxidants: from enzymatic preparation to molecular rationalization, Eur. J. Med. Chem. 127 (2017) 263–274.

[42] M.A. Balbino, M.M.T. de Menezes, I.C. Eleoterio, A.A. Saczk, L.L. Okumura, H. M. Tristao, M.F. de Oliveira, Voltammetric determination of delta 9-THC in glassy carbon electrode: an important contribution to forensic electroanalysis, Forensic Sci. Int. 221 (2012) 29–32.

[43] M. Pyszkova, M. Biler, D. Biedermann, K. Valentova, M. Kuzma, J. Vrba, J. Ulrichova, R. Sokolova, M. Mojovic, A. Popovic-Bijelic, M. Kubala, P. Trouillas, V. Kren, J. Vacek, Flavonolignan 2,3-dehydroderivatives: preparation, antiradical and cytoprotective activity, Free Radic. Biol. Med. 90 (2016) 114–125.

[44] R. Nissim, R.G. Compton, Absorptive stripping voltammetry for cannabis detection, Chem. Cent. J. 9 (2015).

[45] I. Novak, M. Mlakar, S. Komorsky-Lovric, Voltammetry of immobilized particles of cannabinoids, Electroanalysis 25 (2013) 2631–2636.

[46] J. Mazina, A. Spiljova, M. Vaher, M. Kaljurand, M. Kulp, A rapid capillary electrophoresis method with LED-induced native fluorescence detection for the analysis of cannabinoids in oral fluid, Anal. Methods 7 (2015) 7741–7747.

[47] M.F. Wempe, A. Oldland, N. Stolpman, T.H. Kiser, Stability of dronabinol capsules when stored frozen, refrigerated, or at room temperature, Am. J. Health Syst. Pharm. 73 (2016) 1088–1092.

[48] R.M. White, Instability and poor recovery of cannabinoids in urine, oral fluid, and hair, Forensic Sci. Rev. 30 (2018) 33–49.

[49] X. Li, Y.R. Lee, Efficient and novel one-pot synthesis of polycycles bearing cyclols by FeCl3-promoted [2 + 2] cycloaddition: application to cannabicyclol, cannabicyclovarin, and ranhuadujuanine A, Org. Biomol. Chem. 12 (2014) 1250–1257.

[50] L. Crombie, R. Ponsford, A. Shani, B. Yagnitinsky, R. Mechoulam, Hashish components. Photochemical production of cannabicyclol from cannabichromene, Tetrahedron Lett. 9 (1968) 5771–5772.

[51] J. Vacek, J. Ulrichova, B. Klejdus, V. Simanek, Analytical methods and strategies in the study of plant polyphenolics in clinical samples, Anal. Methods 2 (2010) 604–613.

[52] N. Jikomes, M. Zoorob, The cannabinoid content of legal cannabis in Washington state varies systematically across testing facilities and popular consumer products, Sci. Rep. 8 (2018) 4519.

[53] J.T. Wilson, C.A. Fief, K.D. Jackson, S.L. Mercer, J.E. Deweese, HU-331 and oxidized cannabidiol act as inhibitors of human topoisomerase IIalpha and beta, Chem. Res. Toxicol. 31 (2018) 137–144.

[54] M. Renaud-Young, R.M. Mayall, V. Salehi, M. Goledzinowski, F.J.E. Comeau, J. L. MacCallum, V.I. Birss, Development of an ultra-sensitive electrochemical sensor for delta-9 -tetrahydrocannabinol (THC) and its metabolites using carbon paper electrodes, Electrochim. Acta 307 (2019) 351–359.

[55] A.G. Granja, F. Carrillo-Salinas, A. Pagani, M. Gomez-Canas, R. Negri, C. Navarrete, M. Mecha, L. Mestre, B.L. Fiebich, I. Cantarero, M.A. Calzado, M.L. Bellido, J. Fernandez-Ruiz, G. Appendino, C. Guaza, E. Munoz, A cannabigerol quinone alleviates neuroinflammation in a chronic model of multiple sclerosis, J. Neuroimmune Pharmacol. 7 (2012) 1002–1016.

[56] K. Watanabe, N. Usami, I. Yamamoto, H. Yoshimura, Inhibitory effect of cannabidiol hydroxy-quinone, an oxidative product of cannabidiol, on the hepatic microsomal drug-metabolizing enzymes of mice, J. Pharmacobio-Dyn 14 (1991) 421–427.

[57] S.C. Chew, K.L. Nyam, Oxidative stability of microencapsulated kenaf seed oil using Co-extrusion Technology, J. Am. Oil Chem. Soc. 93 (2016) 607–615.

[58] V. Raikos, G. Duthie, V. Ranawana, Denaturation and oxidative stability of hemp seed (*Cannabis sativa* L.) protein isolate as affected by heat treatment, Plant Foods Hum. Nutr. (Dordr.) 70 (2015) 304–309.

[59] S. Uluata, N. Ozdemir, Antioxidant activities and oxidative stabilities of some unconventional oilseeds, J. Am. Oil Chem. Soc. 89 (2012) 551–559.

[60] C. Lipina, H.S. Hundal, Modulation of cellular redox homeostasis by the endocannabinoid system, Open Biol. 6 (2016) 150276.

[61] J. Egea, I. Fabregat, Y.M. Frapart, et al., European contribution to the study of ROS: a summary of the findings and prospects for the future from the COST action BM1203 (EU-ROS), Redox Biol. 13 (2017) 94–162.

[62] E. Hermankova, M. Zatloukalova, M. Biler, R. Sokolova, M. Bancirova, A.G. Tzakos, V. Kren, M. Kuzma, P. Trouillas, J. Vacek, Redox properties of individual quercetin moieties, Free Radic. Biol. Med. 143 (2019) 240–251.

[63] A.M. Chiorcea-Paquim, T.A. Enache, E. De Souza Gil, A.M. Oliveira-Brett, Natural phenolic antioxidants electrochemistry: towards a new food science methodology, Compr. Rev. Food Sci. Food Saf. 19 (2020) 1680–1726.

[64] L. Casares, V. Garcia, M. Garrido-Rodriguez, E. Millan, J.A. Collado, A. Garcia-Martin, J. Penarando, M.A. Calzado, L. de la Vega, E. Munoz, Cannabidiol induces antioxidant pathways in keratinocytes by targeting BACH1, Redox Biol. 28 (2020) 101321.

[65] S. Atalay, I. Dobrzynska, A. Gegotek, E. Skrzydlewska, Cannabidiol protects keratinocyte cell membranes following exposure to UVB and hydrogen peroxide, Redox Biol. 36 (2020) 101613.

[66] P. Gohad, J. McCoy, C. Wambier, M. Kovacevic, M. Situm, A. Stanimirovic, A. Goren, Novel cannabidiol sunscreen protects keratinocytes and melanocytes against ultraviolet B radiation, J. Cosmet. Dermatol. (2020), https://doi.org/10.1111/jocd.13693 in press.

[67] A. Gegotek, S. Atalay, P. Domingues, E. Skrzydlewska, The differences in the proteome profile of cannabidiol-treated skin fibroblasts following UVA or UVB irradiation in 2D and 3D cell cultures, Cells 8 (2019) 995.

[68] H.Y. Wu, C.H. Huang, Y.H. Lin, C.C. Wang, T.R. Jan, Cannabidiol induced apoptosis in human monocytes through mitochondrial permeability transition pore-mediated ROS production, Free Radic. Biol. Med. 124 (2018) 311–318.

[69] P. Schonhofen, L.M. de Medeiros, I.J. Bristot, F.M. Lopes, M.A. De Bastiani, F. Kapczinski, J.A.S. Crippa, M.A.A. Castro, R.B. Parsons, F. Klamt, Cannabidiol exposure during neuronal differentiation sensitizes cells against redox-active neurotoxins, Mol. Neurobiol. 52 (2015) 26–37.